Machining Integration with 5-Axis Articulated Vertical Robots: Simulation and Analytical Modeling

John O'Brien*[1], Claire McCarthy[2] & Patrick Fitzgerald[3]

[1](Associate Professor), School of Biomedical Engineering, University College Dublin, Ireland
[2](Senior Researcher), Department of Materials Science, Trinity College Dublin, Ireland
[3](Head of Department), Mechanical Engineering Division, Cork Institute of Technology, Ireland

ABSTRACT

This paper describes simulation modeling and analysis identification of 5-axis articulated vertical robot for machining integration applications. The standard methodology for the calculation of Cartesian house compliance supported joint compliances and Jacobian matrix is swollen and used for experimental 5-axis machining mechanism. Analytical analysis was conducted for effects of compliances of every joint separately on Cartesian house mechanism compliance. Through an experiment, the Cartesian house compliance is obtained by direct measuring of absolutely the displacements elicited by static forces on 3- orthogonal directions at the tool basketball shot the mechanism space for the case of 3-axis machining.

KEYWORDS: robot, machining, compliance modeling

I. INTRODUCTION

Industrial robots are promising cost-effective and flexible alternative for certain multi-axis milling applications. Compared to machine tools, robots are cheaper and more flexible with larger workspace. It is well known that poor accuracy, stiffness and complexity of programming are the most important limiting factors for wider adoption of robotic machining in machine shops [1]. In order to contribute to efficient use of robots for machining applications, research and development of reconfigurable robotic machining system were initiated [2]. The research and development comprise two groups of problems: the realization of a specialized 5-axis machining robot with integrated motor spindle in order to improve robotic machining accuracy, and the development of the machining robot control and programming system which can be directly used by CNC machine tool programmers and operators [2].

This paper describes analytically and experimentally based compliance modeling and analysis of 5-axis machining robot. The conventional method for the calculation of Cartesian space compliance based on joint compliances and Jacobian matrix [3-5] is expanded and used. Analytical analysis was conducted for effects of compliances of each joint individually on Cartesian space robot compliance. Experimentally, the Cartesian space compliance is obtained by direct measurement of the absolute displacements evoked by static forces along 3- Cartesian directions at the tool tip in the robot workspace for the case of 3-axis milling.

II. PROBLEM STATEMENT

A basic module of the proposed concept of the robotic machining system [5] is the specialized 5-axis robot, Fig. 1a, with integrated motor spindle and with larger workspace, higher payload and stiffness.
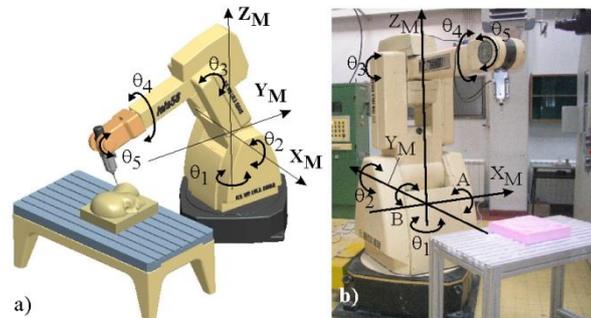

Fig.1. 5-axis machining robot

Due to its advantages in respect of stiffness and singularities, such robot would operate as a specific vertical 5-axis milling machine (X, Y, Z, A, B) spindle-tilting type. The development of specialized 5-axis vertical articulated machining robot is a joint project with robot manufacturer. For the development of control and programming system as well as for the analysis and development of the mechanical structure of 5-axis

machining robot from Fig. 1a, a 6-axis vertical articulated robot with payload of 50kg, Fig. 1b, was used as a testbed, in a way that the sixth axis was blocked. The robot is equipped with high speed motor spindle with maximum speed of 18,000 min^{-1}.

The focus of current research, one part of results being presented in this paper, is related to compliance modelling and analysis of the experimental 5-axis machining robot, which includes:
- Analytically based robot compliance modeling.
- Experimentally based robot compliance modeling.
- Machining experiments.

III. JACOBIAN MATRIX AND WORKSPACE

As it was mentioned, the 5-axis robot from Figure 1a will be considered below as a specific configuration of the 5-axis vertical milling machine (X, Y, Z, A, B) spindle-tilting type. Figure 2 represents a geometric model of the robot.
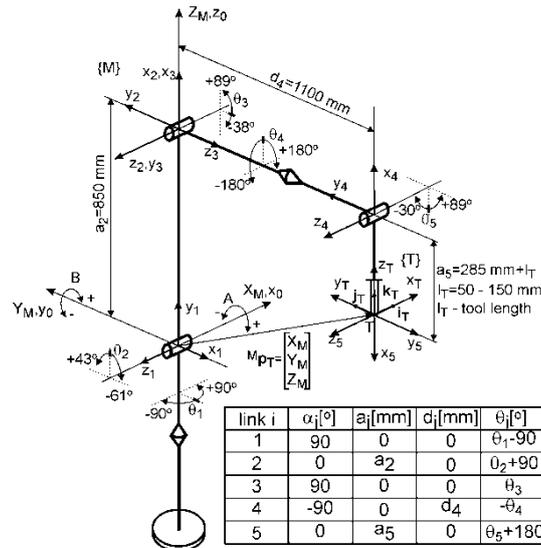

link i	α_j[°]	a_j[mm]	d_j[mm]	θ_j[°]
1	90	0	0	θ_1-90
2	0	a_2	0	θ_2+90
3	90	0	0	θ_3
4	-90	0	d_4	-θ_4
5	0	a_5	0	θ_5+180

Fig.2. D-H link coordinate frames and kinematic parameters

The robot reference frame {M} has been adopted according to the standard of this machine type and coincides with the robot based frame (x_0, y_0, z_0). The tool frame {T} is attached to the milling tool tip T in a way that axis z_T coincides with tool axis and also coincides with axis of the last link of the robot to which motor spindle is attached. The thus configured machining robot, where machining is performed on a work table in front of the robot as well as limited motions in joints relative to the reference position allows for: taking into account only one solution of inverse kinematic, avoiding the robot singularities, conveniences related to the stiffness.

Joint coordinates vector for this 5-axis vertical articulated robot is represented as $\mathbf{\theta} = \begin{bmatrix} \theta_1 & \theta_2 & \theta_3 & \theta_4 & \theta_5 \end{bmatrix}^T$ where θ_i are scalar joint variables controlled by actuators. Given that the robot has 5 DOF, only the direction of tool axis z_T is controllable, while axes x_T and y_T will have uncontrollable rotation about it. The position and orientation of the tool frame {T} relative to robot reference frame {M} is described by world coordinates vector expressed as $\mathbf{x} = \begin{bmatrix} X_M & Y_M & Z_M & A & B \end{bmatrix}^T$.

To model the robot, the Denavit-Hartenberg (D-H) notation [6] was used. To perform kinematic analysis, first coordinate frames are rigidly attached to each link. The homogeneous transformation describing the relation between one link and the next link is traditionally referred to as an A matrix. Matrix $_i^{i-1}A$ designates D-H transformation matrix relating frame (i) to frame ($i-1$). Figure 2 shows D-H coordinate frames and link kinematic parameters for the experimental 5-axis robot from Figure 1b i.e. Figure 2 in the reference position taking into account the ranges of joint motions.

After the D-H coordinate frame is assigned to each link, the transformation between successive frames ($i-1$) and (i) is described as follows:

$$^{i-1}_{i}A = Rot(z,\theta_i)\cdot Trans(z,d_i)\cdot Trans(x,a_i)\cdot Rot(x,\alpha_i)=$$

$$=\begin{bmatrix} ^{i-1}\mathbf{i}_i & ^{i-1}\mathbf{j}_i & ^{i-1}\mathbf{k}_i & ^{i-1}\mathbf{p}_{Oi} \\ \hline 0 & 0 & 0 & 1 \end{bmatrix} \qquad (1)$$

Substituting D-H parameters of the links in equation (1) the transformation matrices $^{i-1}_{i}A$ are obtained first. As noticeable from Figure 2 the frame {T} can be described relative to the frame (x_5,y_5,z_5) by homogeneous transformation matrix as $^5_T T$ [2]. Now, as it is well-known [6], the tool position and orientation i.e. the position and orientation of frame {T} with respect to the robot reference frame {M}, Figure 2, for the given joint coordinates vector $\boldsymbol{\theta}$ and specified link parameters can be determined as

$$^M_T T =^0_1 A\cdot^1_2 A\cdot^2_3 A\cdot^3_4 A\cdot^4_5 A\cdot^5_T T \qquad (2)$$

The position and orientation of arbitrary frame i attached to the link i with respect to the robot reference frame {M} i.e. robot based frame (x_0,y_0,z_0) can be expressed as

$$O=^M_i T=^0_1 A\cdot^1_2 A\cdots^{i-1}_{i}A = \prod_{j=1}^{i}{}^{j-1}_{j}A = \begin{bmatrix} ^{i-1}\mathbf{i}_i & ^{i-1}\mathbf{j}_i & ^{i-1}\mathbf{k}_i & ^{i-1}\mathbf{p}_{Oi} \\ \hline 0 & 0 & 0 & 1 \end{bmatrix} \qquad (3)$$

For $i = 1,2,3,...,n = 5$ where n is number of joints.

The robot Jacobian matrix relates joint velocities to Cartesian velocities of the tool tip. The mapping between static forces applied to the end-effector and resulting torques at the joints can also be described by Jacobian matrix [6,9]. Considering that the robot consists of five revolute joints, the Jacobian matrix has as many rows as there are degrees of freedom and the number of columns is equal to the number of joints

$$J =\begin{bmatrix} J_1 & J_2 & ... & J_n \end{bmatrix} \qquad (4)$$

With column vectors

$$J_i =\begin{bmatrix} ^i\mathbf{k}_{i-1}\times\left(^0\mathbf{p}_n-^0\mathbf{p}_i\right) \\ ^0\mathbf{k}_{i-1} \end{bmatrix} \qquad (5)$$

Substituting vectors from equation (3) in equation (5) Jacobian matrix columns J_i, $i = 1,2,3,...,n = 5$ are obtained.
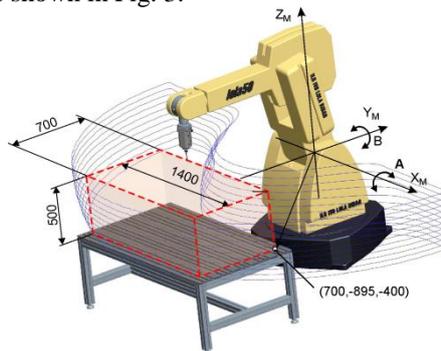
Workspace for 3-axis machining is shown in Fig. 3.

Fig.3. Workspace in the case of 3-axis machining
(A=0º, B=0⁰)

IV.   COMPLIANCE MODELING

As stated in [1, 5, 7, 8] elastic properties of robot segments are insignificant, so there follows below the analysis of compliance model in Cartesian space based on joint compliances. The analysis will be conducted on the existing experimental machining robot from Fig. 1b.

Based on the principle of virtual work, the convectional formulation for the mapping of joint compliance matrix C_θ into the Cartesian space compliance matrix $C_X(\boldsymbol{\theta})$ [3-5] is expressed as

$$C_X(\boldsymbol{\theta}) = J(\boldsymbol{\theta}) \cdot C_\theta \cdot J(\boldsymbol{\theta})^T \qquad (6)$$

Where C_θ is the compliance matrix in joint space which has the diagonal form as

$$C_\theta = diag(C_{\theta 1},...,C_{\theta n}) \qquad (7)$$

and $J(\boldsymbol{\theta})$ is Jacobian matrix.

Equation 6 is practically used in [4] to determine the robot compliance center and in [5] for machining robot compliance analysis where it is stated how suitable it is, for it allows mapping of the joint compliance matrix C_θ into Cartesian compliance matrix $C_X(\boldsymbol{\theta})$ without calculating any inverse kinematic functions. Since C_θ is diagonal, the Cartesian space compliance matrix $C_X(\boldsymbol{\theta})$, Eq. 6, is the sum of the joint compliances associated with each individual joint as

$$C_X(\boldsymbol{\theta}) = C_{X1}(C_{\theta 1}) + ... + C_{Xn}(C_{\theta n}), \; n = 5 \qquad (8)$$

Where

$$C_{Xi}(C_{\theta i}) = C_{\theta i} \cdot \mathbf{J}_i \cdot \mathbf{J}_i^T, \; i = 1,2,...,n, \, n = 5 \qquad (9)$$

While $\mathbf{J}_i$ are column vectors of Jacobian matrix $J(\boldsymbol{\theta})$.

Equations 8 and 9 provide insight into the impact of compliance of each joint individually on the Cartesian space compliance. This means that impact of the corresponding joint is obtained incorporating in the Eq. 8 only its compliance, while the other joints are considered stiff. This is of crucial importance for the present paper, because it can be useful for robot manufacturer's experts in the design of specialized machining robot.

For an articulated robot, $C_X(\boldsymbol{\theta})$ is symmetric non-diagonal and configuration dependent matrix. Thus, if C_θ can be experimentally determined, the Cartesian space compliance matrix C_X, Eq. 6 and the linear displacement of robot tool tip under external static force vector $\mathbf{F} = \begin{bmatrix} F_x & F_y & F_z \end{bmatrix}^T$ at any location in the workspace can be estimated as

$$\delta\mathbf{x} = C_X(\boldsymbol{\theta}) \cdot \mathbf{F} \qquad (10)$$

Table 1 shows the experimentally identified compound joint compliances.

Table 1. Experimentally identified joint compliances

Joint number i	1	2	3	4	5
$C_{\theta i}$[rad/Nm]$\cdot 10^{-7}$	7.14	10.12	12.30	17.32	91.35

Using experimentally determined compound joint compliances, the Cartesian space compliance matrix is calculated in workspace shown in Fig. 3.

Figure 4 shows the distributions of analytically determined compliances in the $Z_M = 0$ plane.
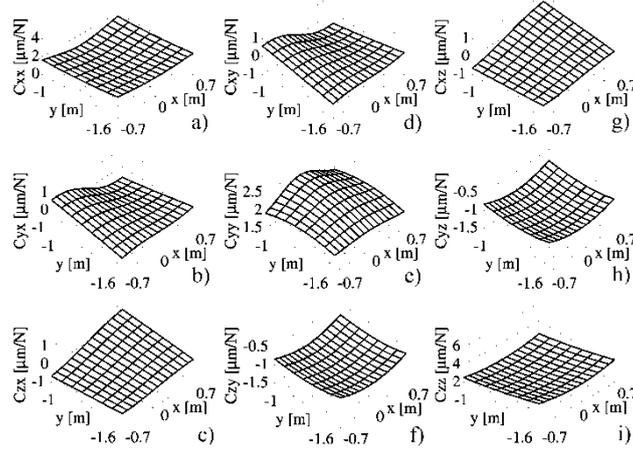
Fig.4. Distributions of analytical compliances in the plane $Z_M=0$

The distributions of direct-compliances C_{xx}, C_{yy} and C_{zz} are presented in Figs. 4a, 4e and 4i respectively. The distributions of cross-compliances C_{yx}, C_{zx} and C_{zy} are given in Figs. 4b, 4c and 4f respectively. Figure 4 can be also viewed as the Cartesian space compliance matrix $C_X(\mathbf{\theta})$ in the $Z_M = 0$ plane in the workspace shown in Fig. 3.

The distributions of dominant components of direct-compliances originating from individual joints are shown in Fig. 5.
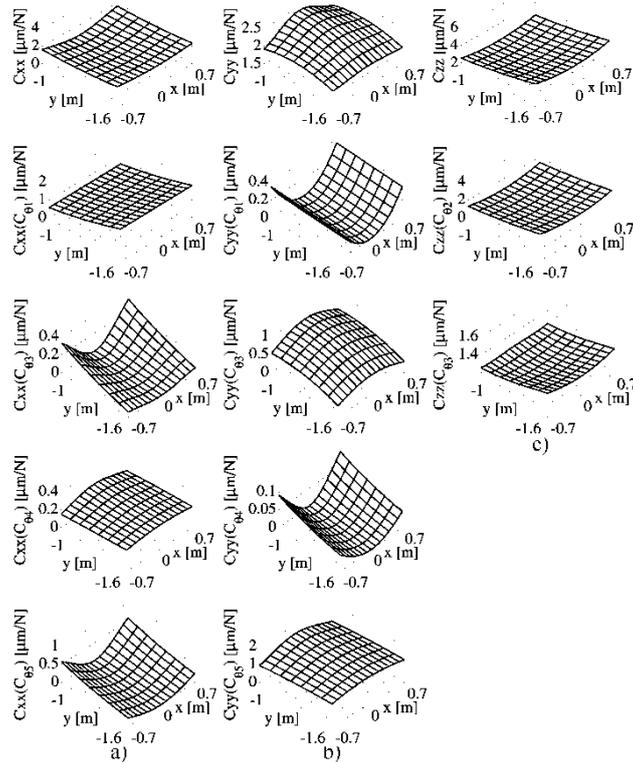

Fig.5. Distributions of dominant direct-compliances components

V. EXPERIMENTAL COMPLIANCE

Another approach to obtain the Cartesian compliance of the machining robot is the direct measurement of the absolute displacement evoked by a load at the tool tip.

The elements of the experimental setup are shown in Fig. 6. The original and deformed positions of sphere-tip tool caused by deadweight of 250N are measured with FARO Portable CMM 3D, from which translational displacements $\delta x, \delta y$ and δz are calculated.

Displacements of the sphere-tip tool are measured in the workspace shown in Fig. 3 at 40 points with the fixed X_M- and Y_M-coordinates in 6 Z_M-levels ($Z_M = -400mm$ to $Z_M = 100mm$). Experimental compliances are determined based on sphere-tip tool displacements evoked by static amount of the milling force of 250N in all 3 Cartesian directions. Figure 6 shows an example of displacements measurement for the case of robot loading in $Y_M -$ direction.
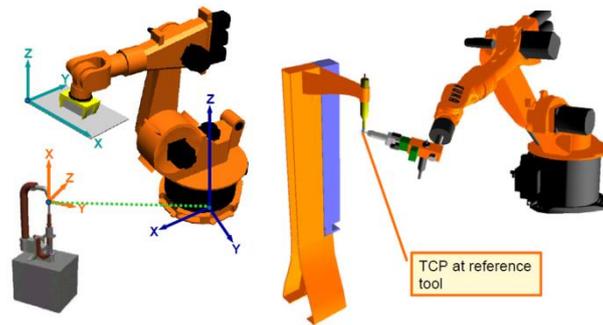

Fig.6. Experimental setup of robot loading and displacements measurement

Figure 7 shows the distributions of experimentally obtained compliances in the $Z_M = 0$ plane. The distributions of experimental direct-compliances C_{xx}, C_{yy} and C_{zz} are shown in Figs. 7a, 7e and 7i, respectively.
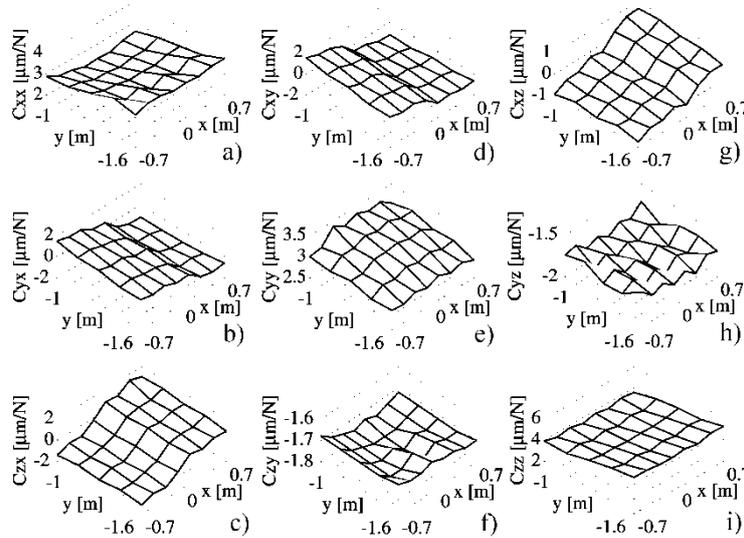

Fig.7.Distributions of experimental compliances in the plane Z_M=0

Experimental cross-compliances are presented in Figs. 7b, 7c and 7f, respectively. Comparing them with analytically determined compliances, Fig. 4, it can be inferred that the character of their distributions is similar, but experimentally determined compliances are slightly higher. Higher values of experimentally determined compliances compared to those determined analytically originate from compliances of structure elements, motor spindle and tool itself.

VI.   CONCLUSION

The paper presents analytically and experimentally based compliance simulation, modeling and analysis of 5-axis machining robot based on conventional approach for the mapping of joint compliances into robot Cartesian space compliance. By expanding this modeling approach, it has been shown that it is possible to analyze each joint compliance impact on robot Cartesian space compliance. Satisfactory correlation between analytically and experimentally determined robot Cartesian space compliances confirms the usability of each joint compliance

effects on tool tip displacements. Suitable model of the process forces and compliance model proposed in this paper also enable the development of virtual robotic machining system for further research. The present research has laid foundations for an advanced design method for one machining robot as well as for the development of strategy for real-time tool tip displacement compensation based on captured process forces.

VII.   REFERENCES

[1] PAN, Z., ZHANG, H. (2017) *Robotics machining from programming to process control: a complete solution by force control*. Industrial Robot: An International Journal, Vol. 35, No 5, pp 400-409

[2] MILUTINOVIC, D., GLAVONJIC, M., SLAVKOVIC, N., DIMIC, Z., ZIVANOVIC, S., KOKOTOVIC, B., TANOVIC, LJ. (2016) *Reconfigurable robotic machining system controlled and programmed in a machine tool manner*. Int J Adv Manuf Technol, Vol.53, No 9-12, pp 1217-1229

[3] HUDGENS, J.C., HERNANDEZ, E., TESAR, D. (2014) *A compliance parameter estimation method for serial manipulator DSC*. Applications of Modeling and Identification to Improve Machine Performance ASME, Vol. 29, pp 15–23

[4] MILUTINOVIC, D., MILACIC, V. (1996) *Micro Scara Robot as Universal Adaptive Compliant Wrist*. Annals of the CIRP, Vol.45, No1, pp 31-34

[5] ABELE, E., WEIGOLD, M., ROTHENBUCHER, S. (2017) *Modeling and identification of an industrial robot for machining applications.* Annals of the CIRP Vol. 56, No1, pp 387-390

[6] CRAIG, J.J. (1989) *Introduction to robotics: mechanics and control, 2nd ed*. Addison - Wesley

[7] ABELE, E., ROTHENBUCHER, S., WEIGOLD, M. (2008) *Cartesian compliance model for industrial robots using virtual joints,* Prod. Eng. Res. Devel Vol. 2, No3, pp 339-343

[8] ALICI, G., SHIRINZADEH, B. (2015) *Enhanced Stiffness Modeling, Identification and Characterization for Robot Manipulators*, IEEE Trasanctions on Robotics, Vol. 21, No 4, pp 554-564

[9] SCIAVICCO, L., SICILIANO, B. (2012) *Modelling and Control of Robot Manipulators, 2nd ed*. Springer-Verlag.